www.sciencevision.info

Research Note

Sci Vis 11 (2), 96-101
April-June, 2011
ISSN (print) 0975-6175
ISSN (online) 2229-6026

A simple study of surface effect in photoassisted field emission by using the Transfer Hamiltonian scheme: application to tungsten

Rosangliana[1] *, Lalmuanpuia[2] and R. K. Thapa[2]

[1] *Department of Physics, Govt. Zirtiri Residential Science College, Aizawl 796 001, India*
[2] *Department of Physics, Mizoram University, Aizawl 796 009, India*

Received 7 April 2011 | Accepted 17 May 2011

ABSTRACT

We present here a model calculation of photoassisted field emission current (PFEC) from tungsten. Transfer Hamiltonian method was used for calculating the transition probability. Matrix element for the transition probability was calculated by using the wavefunctions which are deduced by applying the Kronig-Penney potential model.

Key words: Photofield emission; photofield emission current; transfer Hamiltonian; vector potential; wavefunctions.

PACS No. 73.20.-r, 73.30.+y, 79.70.+q

INTRODUCTION

Photoassisted field emission is a technique in which a metal is irradiated by an incident laser radiation of photon energy ($\hbar\omega$). Photon energy is usually less than the work function (ϕ) of the metal. The incident radiation photoexcites the electrons to states which lies between the Fermi level and the vacuum level, hence these electrons are confined within the metal surface. A strong static electric field ($\sim 10^{11}$ V/m) when applied to the surface of the metal causes the photoexcited electrons to tunnel through the surface potential barrier into the surrounding vacuum. These electrons which are now emitted into the vacuum region constitute the measurable current called photoassisted field emission current (PFEC). For the evaluation of PFEC, the initial state wavefunction as deduced Thapa and Kar[1] by using the Kronig-Penney potential model will be used. Dielectric model proposed by Bagchi and Kar[2] is used for obtaining the vector potential of interest. Calculated PFEC results is compared with the others theoretical and experimental results.[3,4]

Corresponding author: Rosangliana
Phone. +91-9436151667
E-mail: rslct@rediffmail.com

THEORY

A *p*-polarized radiation of photon energy

$\hbar\omega$ is incident on an electron lying at energy E_i below the Fermi level (Fig. 1). This incident radiation usually a laser beam causes the transition of electron from the initial state ψ_i to the final state ψ_f. As this electron still lies below the vacuum level, a high electric field will now cause the electron to be transmitted through the potential barrier to vacuum region thereby causing photoassisted field emission. This happens as the high static field causes the reduction of the work function of the metal causing Schottky effect which brings in the image rounded barrier (IRB). This will reduce the height of the step potential and the work function at the surface as shown in Figure 1, thereby causing tunneling of electrons easier.

The photoassisted field emission current density formula by using Transfer Hamiltonian method is given by

$$\frac{dj(E)}{dE} = \frac{2\pi e}{\hbar}\left|\langle n|-eFz\theta(z)|E_L\rangle\right|^2 D(W)\,\delta$$

$$\left(E_n - E_L\right)\delta\left(E - E_L\right) f\left(E_L\right) \qquad (1)$$

where, *D(W)* is the transmission probability between the two states H_L *and* H_R, and $\left|\langle n|-eFz\theta(z)|E_L\rangle\right|$ is the matrix element due to the transition from (initial to final state) left to right Hamiltonian. $f(E_L)$ is the Fermi-Dirac distribution function, the energy of photoexcited electrons

$$E = W + \frac{\hbar^2 k_{\parallel}^2}{2m}$$

Due to the incident laser radiation, the perturbation term in Eq. (1) is changed to

$$M_{fi} = \left|\langle n|-eFz\theta(z) - \frac{e^2}{4z} + H^{'}|E_L\rangle\right|$$

$$= \frac{\hbar^2}{2m}\left[\int_{-\infty}^{+\infty}\left(\chi_n^*\frac{\partial\psi_{E_L}}{\partial z} - \psi_{E_L}\frac{\partial\chi_n^*}{\partial z}\right)ds - \frac{e^2}{4}\sum_{L,n}\left|\langle n|\left(\frac{1}{z}\right)|E_L\rangle\right| + \sum_{L,n}\left|\langle n|H^{'}|E_L\rangle\right|\right]$$

Figure 1. Model potential used in photofield emission calculations for describing the

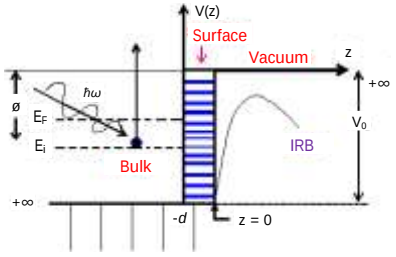

$$= \frac{\hbar^2}{2m}\left[\int_{-\infty}^{+\infty}\left(\chi_n^*\frac{\partial\psi_{E_L}}{\partial z} - \psi_{E_L}\frac{\partial\chi_n^*}{\partial z}\right)ds - \frac{e^2}{4}\int_{-\infty}^{+\infty}\chi_n^*\left(\frac{1}{z}\right)\psi_{E_L}dz + \int_{-\infty}^{+\infty}\chi_n^*\left(H^{'}\right)\psi_{E_L}dz\right]$$

$$\therefore M_{fi} = \frac{\hbar^2}{2m}\int_{-\infty}^{+\infty}\left[\psi_f^*\frac{\partial\psi_i}{\partial z} - \psi_i\frac{\partial\psi_f^*}{\partial z}\right]ds - \frac{\hbar^2 e^2}{8m}\int_{-\infty}^{+\infty}\left[\psi_f^*\left(\frac{1}{z}\right)\psi_i\right]dz + \frac{\hbar^2}{2m}\int_{-\infty}^{+\infty}\left[\psi_f^*\left(A_\omega(z)\frac{d}{dz} + \frac{1}{2}\frac{dA_\omega(z)}{dz}\right)\psi_i\right]dz \qquad (2)$$

here, χ_n^* = wave function of an electron in the final state ψ_f and, ψ_{E_L} = wave function of an electron in the initial state ψ_i.

Initial state wave function ψ_i is obtained by solving the Schrödinger's in the surface region of the metal for which the one dimensional Kronig-Penny potential is used. $A_\omega(z)$ is the one dimensional vector potential of the incident radiation. We are considering the photoassisted field emission to take place along *z*-axis which is normal to the surface.

As shown in Figure 1, the effective potential is given by

$$V(z) = V_o - eFz - \frac{e^2}{4z}$$

where V_0 is the height of the potential barrier, *F* is the applied high electric field and $-\frac{e^2}{4z}$ is the image potential.

Initial state wavefunction ψ_i will be the one deduced by Thapa and Kar[1] by using the Kronig-Penney potential model. This is given in one dimension as

$$\psi_i(z)=\begin{cases}\left(\frac{m}{2\pi\hbar^2k_i}\right)^{\frac{1}{2}}\left[\left(1-iPe^{-i\delta}\sin\delta\right)e^{ik_iz}-\left(P-ie^{i\delta}\sin\delta\right)e^{-ik_iz}\right] & for\ z\le 0\\ \left(\frac{m}{2\pi\hbar^2k_i}\right)^{\frac{1}{2}}Te^{-\chi z} & for\ z>0\end{cases} \tag{3}$$

Imposing the boundary conditions on the above equation gives reflection (*P*) and the transmission coefficients (*T*) as

$$P=\frac{\left(\chi-ik_i\right)-\left(k_i-\chi\right)e^{i\delta}\sin\delta}{\left(\chi-ik_i\right)+\left(k_i-\chi\right)e^{i\delta}\sin\delta}\quad \text{and}$$

$$T=\frac{2k_i\sin 2\delta}{\left(\chi-ik_i\right)+\left(k_i-\chi\right)\sin\delta e^{-i\delta}} \tag{4}$$

Where $\delta=-\tan\left(\frac{\hbar^2k_i}{mg}\right)$ is the phase shift introduced in the transmitted wave and *g* is the strength of the potential. The final state wave function in one dimension is

$$\psi_f(z)=\begin{cases}\left(\frac{m}{2\pi\hbar^2q}\right)^{\frac{1}{2}}\left(\frac{2q}{q+k_f}\right)e^{ik_fz}.e^{-\alpha|z|}, & z\le 0\\ \left(\frac{m}{2\pi\hbar^2q}\right)^{\frac{1}{2}}\left[e^{iqz}+\left(\frac{q-k_f}{q+k_f}\right)e^{-iqz}\right], & z>0\end{cases} \tag{5}$$

Here,

$$k_i=\left(\frac{2mE_i}{\hbar^2}\right)^{\frac{1}{2}}\qquad k_f=\left(\frac{2mE_f}{\hbar^2}\right)^{\frac{1}{2}}$$

$$q=\left[\frac{2m}{\hbar^2}(E_f-V_0)\right]^{\frac{1}{2}}\qquad \chi=\left[\frac{2m}{\hbar^2}(V_0-E_i)\right]^{\frac{1}{2}} \tag{6}$$

where, $E_f=E_i+\hbar\omega\ \ and,\ \ V_0=E_f+\phi$

The one dimensional form of vector potential of interest used in Eq. (2) for the bulk ($z < -d$), surface ($-d \le z \le 0$) and vacuum ($z > 0$) regions are given by

$$A_\omega(z)=\begin{cases}A_1 & for \quad z\le -d\\ A_1.\frac{\varepsilon(\omega)d}{d+\left[1-\varepsilon(\omega)\right]z} & for \quad -d\le z\le 0\\ A_1.\varepsilon(\omega) & for \quad z\ge 0\end{cases} \tag{7}$$

where $A_1=\frac{-\sin 2\theta_i}{\left[\varepsilon(\omega)-\sin^2\theta_i\right]^{1/2}+\varepsilon(\omega)\cos\theta_i}$ (8)

Now, the matrix element in Eq. (2) in one dimension is given by

$$M_{fi}=\frac{\hbar^2}{2m}\left[\int_{-a}^{0}\psi_f^*\frac{d}{dz}\psi_i\,dz+\int_{-a}^{0}\psi_i\frac{d}{dz}\psi_f^*\,dz\right]-\frac{\hbar^2e^2}{8m}\left[\int_{-a}^{0}\psi_f^*\left(\frac{1}{z}\right)\psi_i\,dz\right]+\frac{\hbar^2}{2m}\left[\int_{-a}^{0}\psi_f^*A(z)\frac{d}{dz}\psi_i.dz+\int_{-a}^{0}\psi_f^*\left(\frac{1}{2}\right)\frac{dA(z)}{dz}\psi_i\,dz\right] \tag{9}$$

The transmission probability *D(W)* used in Eq. (1) had been calculated by Thapa and Das,[5] which is given by

$$D(W)=\frac{W^{\frac{1}{4}}\sqrt{\pi}}{(\hbar eF)^{\frac{1}{6}}}\left(\frac{2ik_i}{ik_i+\chi}\right)(2m)^{\frac{1}{12}}\times exp\left[-i\left(\frac{2}{3}\frac{W^{\frac{3}{2}}\sqrt{2m}}{\hbar eF}+\frac{\pi}{4}\right)\right] \tag{10}$$

By using the above equations in Eq. (1), PFEC can be calculated. As all the integrals

when expanded in Eq. (1) cannot be solved analytically, FORTRAN programme are written.

RESULTS AND DISCUSSIONS

We present here the results of PFEC from tungsten obtained by using the transfer Hamiltonian method. PFEC is calculated as a function of applied high static electric field (F), initial state energy (E_i), photon energy ($\hbar\omega$). We have also calculated the matrix element as a function of photon energy. The following data are used for the calculations:

Initial state energy (E_i) = 2.1488 *eV*
Potential barrier height (V_0) = 15 *eV*
Work function (ϕ) = 4.928 *eV*
Fermi energy (E_F) = 10.06 *eV*
Scattering factor (α) = 0.35

The plot of PFEC as a function of the high applied electric field F is shown in Figure 2 for photon energies 1.20 *eV*, 1.96 *eV* and 3.54 *eV* in the case of surface width 58.92 *nm*. For all the photon energies, it is seen that PFEC decreases exponentially as the applied field (F) is gradually increases. We have also plotted PFEC as a function of the applied field for the same photon energies and initial state energy, but for narrow surface width (Fig. 3). In this case, it is seen that PFEC approached

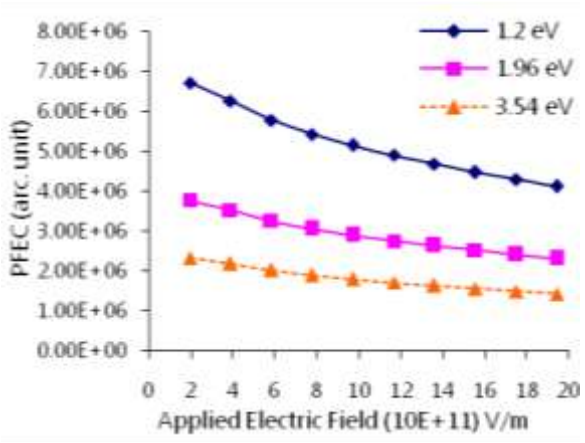

Figure 2. Plot of photofield emission current (PFEC) against applied field F in tungsten for photon energies 1.20 *eV*, 1.96 *eV* and 3.54 *eV*. Initial state energy E_i = 1 *eV* below Fermi level, and angle of incidence of photon radiation is 45°, surface width = 58.92 *nm*.

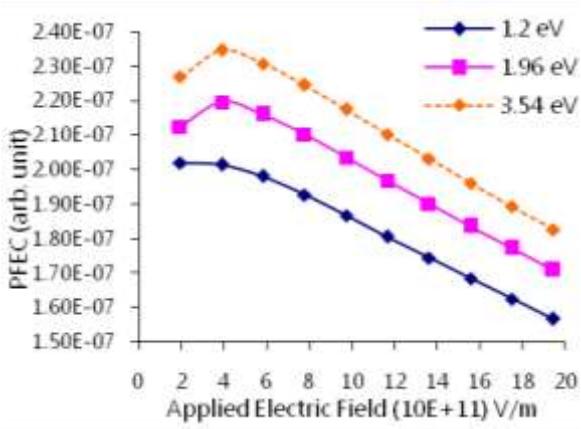

Figure 3. Plot of photofield emission current (PFEC) against applied field F in Tungsten for 1.2 *eV*, 1.96 *eV* and 3.54 *eV* photon energies for narrow surface width. Initial state energy E_i = 1 *eV* below Fermi level, and angle of incidence of photon radiation is 45°.

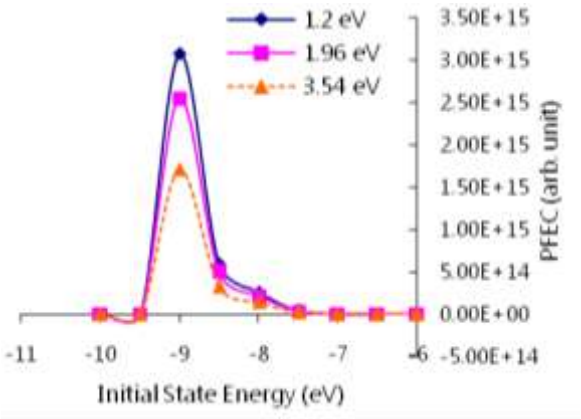

Figure 4. Plot of PFEC against initial state energy E_i below Fermi level (E_F=0.0) in tungsten for photon energies 1.20 *eV*, 1.96 *eV* and 3.54 *eV*. Here value of applied field $F = 3.08 \times 10^{11}$ *V/m* and angle of incidence of photon radiation is 45°, surface width = 58.92 *nm*.

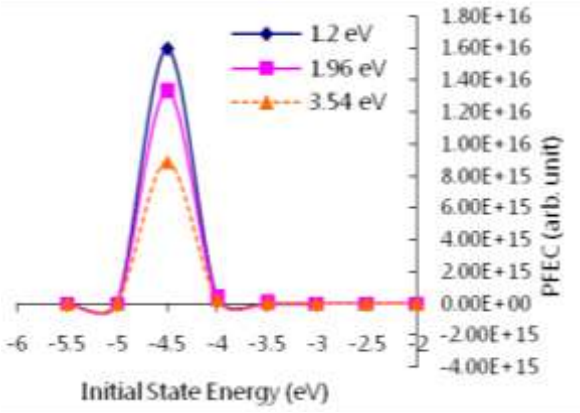

Figure 5. Plot of PFEC against initial state energy E_i below Fermi level (E_F =0.0) in tungsten for photon energies 1.20 *eV*, 1.96 *eV* and 3.54 *eV* for narrow surface width. Here value of applied field $F = 3.08 \times 10^{11}$ *V/m* and angle of incidence of photon radiation is 45°.

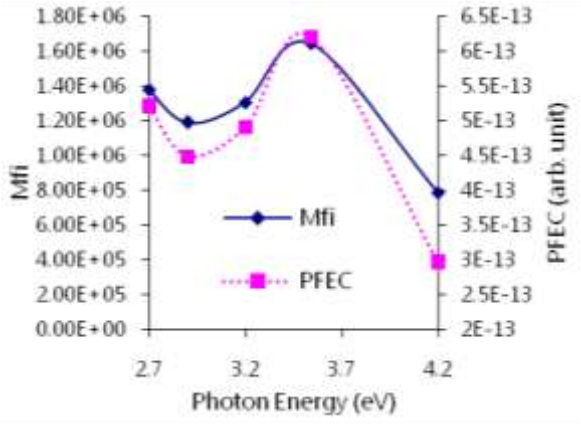

Figure 6. Plot of matrix element M_{fi} and PFEC against photon energy in tungsten for values of applied field $F = 3.08 \times 10^{11}$ *V/m*, initial state energy E_i = 1*eV* Fermi level. The angle of incident photon radiation is 45° and surface width = 58.92 *nm*.

towards a maximum and then decreases with the increase of applied field.

In Figure 4, the variation of PFEC as a function of initial state energy is shown for 1.2 *eV*, 1.96 *eV* and 3.54 *eV* photon energies, respectively. We observed here that PFEC shows maximum peak at E_i = -9 *eV* for all three photon energies. However, height of peak in PFEC for 1.2 e*V* of photon energy is highest. With increase in the initial state energy, the PFEC shows no signals beyond E_i = -7 *eV* of initial state energy when the width of the surface is taken at 58.92 *nm.* Similar features had been also found in the experimental results of Gao and Reifenberger.[4] However in the case of a narrow surface width as shown in Figure 5, but the position of the peak is located at E_i = -4.5 *eV* below the Fermi level.

In Figure 6, we show the results of PFEC and matrix element M_{fi} plotted as a function of photon energy $\hbar\omega$ which is less than the work function $\varnothing$ = 4.928 *eV* (for tungsten). We find from the plots that both PFEC and the matrix element shows maxima at photon energy ($\hbar\omega$ = 3.54 *eV*) with the variation of photon energies.

CONCLUSION

By using the transfer Hamiltonian method for calculating the transition probability, we have shown here the variation of PFEC as a function of various parameters like applied high field, surface thickness, incident photon energies. The variation of PFEC as a function of applied field showed an exponential decrease with the increase of applied field. These features were also observed in the case of tungsten in which the PFEC was calculated by using other methods like free-electron model[6] and group theoretical method.[7] Similar behavior in PFEC was found in the experimental results of Radon *et al.*[8] However, this is also an evidence that there is no oscillations observed in PFEC as found out experimentally by Schwartz and Schaich.[9] We have also done the calculations for the case of narrow surface width by keeping all the parameters

for tungsten are same and the results of PFEC are shown in Figure 3. We find that with the increase of applied field, the PFEC increases and attain a maximum peak, after which it decreases with the further increase of applied field.

The calculations of PFEC as a function of initial state energies showed occurrence of peaks at the same initial state energy that is, at -9.0 *eV* for surface width 58.92 *nm* (Fig. 4) for all the photon energies. However, for the narrow surface width (Fig. 5), the peak shifted towards the Fermi level and occurred at -4.5 *eV* below the Fermi level for all the photon energies. The indication of such shift is that narrowing of surface width plays important role as the contributions are mostly from electrons near the Fermi level.

The behaviour of PFEC and matrix element (M_{fi}) as a function of photon energies is very important as vector potential is included in the formula for PFEC. This is rightly indicated by the almost similar behaviour of PFEC and M_{fi}.

We find from our results that the method of transfer Hamiltonian can also be used in photoassisted field emission studies. The reasons for this being that this approach of studies are also reproducing similar results in the case of tungsten as were obtained by Gao and Reifenberger.[10]

ACKNOWLEDGEMENT

RKT acknowledges a research grant from DAE (BRNS), Mumbai. RSL thanks Department of Physics, Mizoram University for permission to use the computational facilities and a research fellowship from Mizoram Scholarship Board.

REFERENCES

1. Thapa RK & Kar N (1988). Photoemission calculation from band state Kronig-Penney model and spatially varying photon field. *Indian J Pure Appl Phys*, 26, 620.
2. Bagchi A & Kar N (1978). Reflection effects in angle-resolved photoemission from surface states on metal. *Phys Rev*, B18, 5240-5247.
3. Gao Y & Reifenberger R (1986). Photofield emission from transition-metal surface states. *Phys Rev*, B35, 4284-4290.
4. Gao Y & Reifenberger R (1987). Band-structure effects in photofield emission. *Phys Rev,* B35, 6627-6636.
5. Thapa RK & Das G (2005). A simple theory of photofield emission from the surface of a metal. *Int J Mod Phys*, B19, 3141-3149.
6. Rosangliana, Ghimire MP, Lalmuanpuia, Sandeep & Thapa RK (2010). Study of photofield emission in tungsten by using free electron model. *Indian J Phys*, 84, 723-727.
7. Thapa RK, Ghimire MP, Rosangliana, Sandeep & Lalmuanpuia (2010). A model calculation of photofield emission by using a simple vector potential. *Sci Vis*, 10, 31-34.
8. Radon T, Jurczyszyn L & Hadzel P (2002). Size effect in photofield emission from (001) tungsten. *Surf Sci*, 513, 549-554.
9. Schwartz C & Schaich WL (1981). Photostimulated field emission: A theoretical attempt to find rapid oscillations with applied field. *Phys Rev*, B24, 1583.
10. Gao Y & Reifenberger R (1987). Yield of photofield emitted electrons from tungsten. *Phys Rev*, B35, 8301-8307.